International Journal of Chemistry and Materials Research
2015 Vol. 3, No. 1, 17-26.
ISSN(e): 2311-763X
ISSN(p): 2312-0991
DOI: 10.18488/journal.64/2015.3.1/64.1.17.26

THE EXCITED ELECTRONIC STATES AND THE OSCILLATOR STRENGHT CALCULATED FOR FLATTENED CYLINDRICAL $Cd_{1-x}Zn_xS$ QUANTUM DOTS

S. Marzougui[1] --- N. Safta[2]†

[1,2]*Unité de Physique Quantique, Faculté des Sciences, Université de Monastir, Monastir, Tunisia*

ABSTRACT

The present paper is aimed to investigate theoretically the quantum confinement in $Cd_{1-x}Zn_xS$ – related quantum dots with x the atomic fraction of Zn. For both electrons and holes, we have calculated the excited bound states with use of the flattened cylindrical geometry model and assuming a finite potential at the boundary. The confined sub bands have been calculated based on squared quantum well wave – functions. A theoretical analysis is also made to calculate the oscillator strength of inter sub band transitions as a function of zinc composition. The goal of the latter study is to investigate the optical behavior of flattened cylindrical $Cd_{1-x}Zn_xS$ quantum dots.

Keywords: Quantum dots, Flattened cylindrical geometry, Finite potential, $Cd_{1-x}Zn_xS$, Excited bound states, Non volatile memories.

Contribution/ Originality

This study is one of very few studies which have investigated theoretically the electronic and optical properties of $Cd_{1-x}Zn_xS$ quantum dots with a flattened cylindrical geometry. The excited sub bands have been calculated for electrons, heavy holes and light holes. The oscillator strength of inter sub band transitions has also been computed.

1. INTRODUCTION

Films of $Cd_{1-x}Zn_xS$ are attracting considerable interest in both fundamental and applied research [1-5]. In fact, $Cd_{1-x}Zn_xS$ is a wide band gap n – type semiconductor having strong potential as a window material in hetero junction solar cells with a p-type absorber layer like $CuInSe_2$ [6]. Moreover, the $Cd_{1-x}Zn_xS$ is useful for fabricating p – n junctions without lattice mismatch in devices based on quaternary compounds like $CuIn_xGa_{1-x}Se_2$ or $CuSnS_zSe_{1-z}$ [7].

On the subject of quantum dots (QDs) based on the $Cd_{1-x}Zn_xS$ ternary alloy, they are attracting considerable interest in both fundamental and applied research. In the fundamental

† Corresponding author

view point, $Cd_{1-x}Zn_xS$ QDs have specific properties like size quantization, zero – dimensional electronic states, non linear optical behaviour, coupling between QDs etc [6, 8-19]. In technological applications, $Cd_{1-x}Zn_xS$ QDs are of great interest as well. We can cite red-light-emitting diodes (LEDs) fabricated using CdSe/ $Cd_{1-x}Zn_xS$ quantum dots (QDs) [20], blue (~440 nm) liquid laser with an ultra-low threshold achieved by engineering unconventional ternary CdZnS/ZnS alloyed-core/shell QDs [21] and fluorescent CdS QDs used for the direct detection of fusion proteins [22]. Recently, $Cd_{1-x}Zn_xS$ QDs have become one of the most promising materials in solar cell fabrication [23]. The current challenge is, now, to use these QDs for designing a new class of nanostructure devices such as the non - volatile memories [16-19].

Concerning the growth of $Cd_{1-x}Zn_xS$ QDs, there are several methods like the inverted micelles [24], the selective area – growth technique [25], the single source molecular precursors [26], the colloidal method [27] and the Sol gel technique [28]. For characterization experiences made on $Cd_{1-x}Zn_xS$ QDs, we can cite the studies given by Refs.[6, 29, 30].

In a realistic description, the electronic properties of $Cd_{1-x}Zn_xS$ QDs, embedded in a dielectric matrix using the Sol – gel technique, have to be studied using spherical geometry. Based on this model, two approaches have been proposed to illustrate the potential energy, a potential with an infinite barrier [1, 8-10] and a potential with a finite barrier [11, 13] at the boundary. The latter potential has the advantage to predict the coupling between QDs. However, the spherical geometry does not lend simply to calculate the band edges of coupled QDs, especially along different quantization directions. In order to around this difficulty, the $Cd_{1-x}Zn_xS$ QDs have been, in a previous work, studied in such a way that electrons and holes are assumed to be confined in dots having a flattened cylindrical geometry with a finite barrier height at the boundary [12]. As an experimental support, absorption data obtained on $Cd_{1-x}Zn_xS$ nano crystals grown by sol gel technique [6] have been used [12]. More precisely, a fitting, which consisted to oblige the optical band gap to coincide with the effective band gap calculated for $Cd_{1-x}Zn_xS$ QDs, has been made [12]. By restricting this investigation to the ground state, the shape of the confinement potentials, the quantized energies, their related envelope wave – functions and the QDs sizes have been calculated [12].

In the present work, this study is extended to the excited states. Moreover, a peculiar attention is paid for the oscillator strength associated with inter sub band transitions. Calculations will be made versus the ZnS molar fraction. The paper is organized as follows: after an introduction, we present the theoretical formulation. In the following, we report numerical results and discussion. The conclusion is presented in the last part.

2. THEORETICAL FORMULATION

The system to simulate consists of an electron and a hole, both being confined in a $Cd_{1-x}Zn_xS$ QD capped inside a dielectric host matrix. The QD being studied is assumed to having a cylindrical geometry of radius R and a height L. Moreover, we suppose that the diameter is larger than the height in such a way that the quantum confinement along the transversal directions of the cylinder can be disregarded. On the other hand, the electron and hole confinements are

assumed to be uncorrelated. Using these approximations, the problem to solve reduces to that of a one – dimensional potential. Hence, the electron and hole states in a QD are given from the Hamiltonian:

$$H = -\frac{\hbar^2}{2m^*_{e,h}}\frac{d^2}{dz^2_{e,h}} + V_{e,h}\left(z_{e,h}\right) \quad (1)$$

where $\hbar$ is the Plank's constant, m^* is the effective mass of free carriers, z is the direction perpendicular to the QD base and *V(z)* represents the potential energy. The subscripts e and h refer to the electron and hole particles respectively. Based on the flattened cylindrical geometry assumption, *V(z)* can be modeled by a square – shaped potential with a width *L* and a barrier height *V*. In deriving the Hamiltonian *H*, we have adopted the effective mass theory (EMT) and the band parabolicity approximation (BPA) as well. The mismatch of the effective mass between the well and the barrier has been neglected. Therefore, we distinguish two kinds of solutions:

(i) The even states: in this case, the wave functions are given by:

$$\psi_{e,h}(z) = \begin{cases} A_{e,h}\cos\left(\frac{k_{e,h}L}{2}\right)e^{\rho_{e,h}\left(z+\frac{L}{2}\right)} & ; z \le -\frac{L}{2} \\ A_{e,h}\cos k_{e,h}z & ; -\frac{L}{2} \le z \le \frac{L}{2} \\ A_{e,h}\cos\left(\frac{k_{e,h}L}{2}\right)e^{-\rho_{e,h}\left(z-\frac{L}{2}\right)} & ; z \ge \frac{L}{2} \end{cases} \quad (2)$$

with

$$k_{e,h} = \sqrt{\frac{2m^*_{e,h}\ E_{e,h}}{\hbar^2}} \quad (3)$$

$$\rho_{e,h} = \sqrt{\frac{2m^*_{e,h}\ \left(V_{e,h} - E_{e,h}\right)}{\hbar^2}} \quad (4)$$

$$A_{e,h} = \left[\frac{1}{\rho_{e,h}}\cos^2\left(\frac{k_{e,h}L}{2}\right) + \frac{L}{2} + \frac{1}{2k_{e,h}}\sin k_{e,h}L\right]^{-\frac{1}{2}} \quad (5)$$

The confinement energies *E* are deduced from the following equation:

$$\left|\cos\frac{k_{e,h}L}{2}\right| = \frac{k_{e,h}}{k_{0e,h}} \quad (6)$$

with the condition:

$$tg\frac{k_{e,h}L}{2}\rangle 0 \qquad (7)$$

where:

$$k_{0e,h}=\sqrt{\frac{2m^{*}_{e,h}\,V_{e,h}}{\hbar^{2}}} \qquad (8)$$

(ii) The odd states: in this case, the wave functions are given by:

$$\psi_{e,h}(z)=\begin{cases}-C_{e,h}\sin\left(\frac{k_{e,h}L}{2}\right)e^{\rho_{e,h}\left(z+\frac{L}{2}\right)} & ;z\le-\frac{L}{2}\\ C_{e,h}\sin k_{e,h}z & ;-\frac{L}{2}\le z\le\frac{L}{2}\\ C_{e,h}\sin\left(\frac{k_{e,h}L}{2}\right)e^{-\rho_{e,h}\left(z-\frac{L}{2}\right)} & ;z\ge\frac{L}{2}\end{cases} \qquad (9)$$

with

$$C_{e,h}=\left[\frac{1}{\rho_{e,h}}\sin^{2}\left(\frac{k_{e,h}L}{2}\right)+\frac{L}{2}-\frac{1}{2k_{e,h}}\sin k_{e,h}L\right]^{-\frac{1}{2}} \qquad (10)$$

The confinement energies E are deduced from the following equation:

$$\left|\sin\frac{k_{e,h}L}{2}\right|=\frac{k_{e,h}}{k_{0e,h}} \qquad (11)$$

with the condition:

$$\operatorname{cotg}\frac{k_{e,h}L}{2}\langle 0 \qquad (12)$$

In the following, the confinement energies will be noted as: $E_e = E_n$ for the electrons, $E_h = HH_n$ for the heavy holes and $E_h = LH_n$ for the light holes with n = 1, 2 …

The electron band parameters used in the present work are listed (Table 1). These parameters were treated as fitting parameters [12]. Concerning the values of $m^{*}_{lh}(\mathrm{CdS})$ and $m^{*}_{lh}(\mathrm{ZnS})$, we have used, in this work, those given by Ref [14], i.e. 0.7 and 0.23 respectively in free electron mass m_0. For the $Cd_{1-x}Zn_xS$ QDs, the effective masses were calculated using the Vegard's law.

3. RESULTS AND DISCUSSION

3.1. The Electronic States

The relevant values of the HH_2 state for heavy holes and LH_1 state for light holes are illustrated versus the Zn molar fraction (Figure 1). In the latter, we have also plotted the confinement energy HH_1 of the hole ground state taken from Ref. [12]. We have fitted the x – dependence of the hole sub bands by using polynomial laws. The fitting method is based on the origin 8 software. Analytical expressions obtained are summarized (Table 2). As can be noticed from obtained results: (i) the sub bands HH_1, HH_2 and LH_1 shift up in energy as Zn composition increases, (ii) opposite to the ground state HH_1, the excited sub bands HH_2 and LH_1 show a more rapid increasing with the increase of Zn composition. This trend is mainly due to the x-dependence of the barrier potential V_h. Indeed, the latter parameter has been found to increase with increased Zn composition [12].

For electrons, Figure 2 shows the sub band energies calculated as a function of Zn composition. It has been found that: (i) the excited electron state E_2 is resonant up to the composition x = 0.6 (ii) this state is, however, detected as a localized state in the quantum well for the Zn composition range $0.8 \leq x \leq 1$. Since, the well width L being the same and the effective mass m_e^* remains practically unchanged for all Zn compositions, this result is presumably related to the barrier potential height V_e. Indeed, this parameter is found to increase with x [12]. In the Figure 2, we have also plotted the confinement energy of the E_1 electron ground state taken from Ref. [12]. Table 2 reports the x-dependence of this energy.

On the other hand, an analysis of the obtained results for electrons and holes reveals: (i) the hole confinement is not large going from CdS to ZnS, compared to that obtained for the electrons. This trend is mainly due to the large difference between the electron and hole effective masses in CdS, ZnS and in their alloys, (ii) there is an agreement with results obtained from the spherical geometry in terms of the magnitude order [13]. Once again, this confirms, the validity of the flattened cylindrical geometry.

3.2. The Oscillator Strength

Also discussed in the paper is the efficiency of emission in $Cd_{1-x}Zn_xS$ QDs. This characteristic is illustrated by the oscillator strength. For the $Cd_{1-x}Zn_xS$ system being studied, our calculation shows that the oscillator strength is null when the inter band transition corresponds to an electron state and a hole state of a same parity. For the other situations, we can distinguish two cases:

(i) The inter sub band transition happens between an even electron state (*E.E.S*) and an odd hole state (*O.H.S*). In this case, the oscillator strength is given by:

$$f_{E.E.S \to O.H.S} = \frac{2m_0}{\hbar^2}(E_g^{bulk} + E_e + E_h)\left|\langle \psi_e | Z | \psi_h \rangle\right|^2 \quad (13)$$

where E_g^{bulk} is the band gap for bulk $Cd_{1-x}Zn_xS$. Values of this parameter are taken from Ref [31] and reported (Table 3), Z is the one dimensional operator position and

$$\langle\psi_e|Z|\psi_h\rangle = A_eC_h\cos\left(\frac{k_eL}{2}\right)\sin\left(\frac{k_hL}{2}\right)\left(\frac{2}{\alpha^2}+\frac{L}{\alpha}\right)+A_eC_h\left[-\frac{L}{2\beta}\cos\left(\frac{\beta L}{2}\right)+\frac{1}{\beta^2}\sin\left(\frac{\beta L}{2}\right)\right]+A_eC_h\left[-\frac{1}{\gamma^2}\sin\left(\frac{\gamma L}{2}\right)+\frac{L}{2\gamma}\cos\left(\frac{\gamma L}{2}\right)\right] \quad (14)$$

with

$$\alpha = \rho_e + \rho_h$$
$$\beta = k_e + k_h \quad (15)$$
$$\gamma = k_e - k_h$$

This case includes the $E_1 \rightarrow HH_2$ transition.

(ii) The inter sub band transition between an odd electron state (*O.E.S*) and an even hole state (*E.H.S*). The oscillator strength is, then, given by:

$$f_{O.E.S\rightarrow E.H.S} = \frac{2m_0}{\hbar^2}(E_g^{bulk} + E_e + E_h)\left|\langle\psi_e|Z|\psi_h\rangle\right|^2 \quad (16)$$

where

$$\langle\psi_e|Z|\psi_h\rangle = C_eA_h\sin\left(\frac{k_eL}{2}\right)\cos\left(\frac{k_hL}{2}\right)\left(\frac{2}{\alpha^2}+\frac{L}{\alpha}\right)+C_eA_h\left[-\frac{L}{2\beta}\cos\left(\frac{\beta L}{2}\right)+\frac{1}{\beta^2}\sin\left(\frac{\beta L}{2}\right)\right]+C_eA_h\left[\frac{1}{\gamma^2}\sin\left(\frac{\gamma L}{2}\right)-\frac{L}{2\gamma}\cos\left(\frac{\gamma L}{2}\right)\right] \quad (17)$$

This case includes the $E_2 \rightarrow HH_1$ and $E_2 \rightarrow LH_1$ transitions.

Thus, we have calculated the x-dependent oscillator strength for the inter sub band transitions using Eqs. (13) and (16). Typical results, obtained, are shown (Figure 3). As has been found, (i) the variation of $f_{E1\rightarrow HH2}$ presents some fluctuations as x increases in such a way that the values are situated between 4.92 and 13.35 (ii) the magnitude order of $f_{E2\rightarrow LH1}$ is lower than that of $f_{E1\rightarrow HH2}$ and $f_{E2\rightarrow HH1}$ (iii) $Cd_{1-x}Zn_xS$ QDs with high zinc content offer a large efficiency of radiative recombination.

4. CONCLUSION

In summary, we have calculated the discrete energy spectrum of $Cd_{1-x}Zn_xS$ QDs. As a geometry model, we have considered flattened cylindrical QDs with a finite potential barrier at the boundary. For electrons, heavy holes and light holes, we have calculated the excited sub bands by using the one dimensional quantum well eigen functions. We have also computed the oscillator strength of inter sub band transitions. Calculations were extended in the all composition range from CdS to ZnS.

It is worth to notice that computation of excited bound states for electrons and holes is of great interest. Indeed, in $Cd_{1-x}Zn_xS$ QD structures with higher Zn composition, the excited states, if occupied by excited carriers, can favour the multi – level emissions from the confined sub bands. Moreover, the excited carriers states can interact with impurity levels intentionally incorporated,

governing the transport properties of $Cd_{1-x}Zn_xS$ QDs. On the other hand, this study showed that $Cd_{1-x}Zn_xS$ QDs with high zinc content offer a large efficiency of radiative recombination.

REFERENCES

[1] J. Liu, D. Zhang, X. Pu, J. Liu, and R. Zhang, "Combustion synthesis of Zn1−xCdxS and its photodegradation performance of methylene blue," *Materials Letters*, vol. 117, pp. 158-161, 2014.

[2] A. Sakly, N. Safta, and A. Ben Lamine, "Interpretation of the bowing phenomenon in Cd1-xZnxS alloy," *J. Mater. Sci.-Mater. Electron.*, vol. 15, pp. 351-354, 2004.

[3] N. A. Shah, A. Nazir, W. Mahmood, W. A. Syed, S. Butt, Z. Ali, and A. Maqsood, "Physical properties and characterization of Ag doped CdS thin films," *J. Alloys Compd.*, vol. 512, pp. 27–32, 2012.

[4] T. P. Kumar, S. Saravanakumar, and K. Sankaranayanan, "Effect of annealing on the surface and band gap alignment of CdZnS thin films," *Appl. Surf. Sci.*, vol. 257, pp. 1923-1927, 2011.

[5] N. Safta, "Fluctuations mode of the gap as a function of composition of Cd1-xZnxS ternaries," *Ann. Chim. Sci. Mat.*, vol. 29, pp. 105-112, 2004.

[6] B. Bhattacharjee, S. K. Mandal, K. Chakrabarti, D. Ganguli, and S. Chaudhui, "Optical properties of Cd1-xZnxS nanocrystallites in sol–gel silica matrix," *J. Phys. D: Appl. Phys.*, vol. 35, pp. 2636-2642, 2002.

[7] N. Gawedang and T. Gawedang, "Investigations on chemically deposited Cd1-xZnxS thin films with low Zn content," *Materials Letters*, vol. 59, pp. 3577-3584, 2005.

[8] K. K. Nanda, S. N. Sarangi, S. Mohanty, and S. N. Sahu, "Optical properties of CdS nanocrystalline films prepared by a precipitation technique," *Thin Solid Films*, vol. 322, pp. 21-27, 1998.

[9] H. Yükselici, P. D. Persans, and T. M. Hayes, "Optical studies of the growth of Cd1-xZnxS nanocrystals in borosilicate glass," *Phys. Rev. B.*, vol. 52, pp. 11763-11772, 1995.

[10] Y. Kayanuma, "Quantum-size effects of interacting electrons and holes in semiconductor microcrystals with spherical shape," *Phys. Rev. B.*, vol. 38, pp. 9797-9805, 1988.

[11] N. Safta, A. Sakly, H. Mejri, and Y. Bouazra, "Electronic and optical properties of Cd1-xZnxS nanocrystals," *Eur. Phys. J. B.*, vol. 51, pp. 75-78, 2006.

[12] N. Safta, A. Sakly, H. Mejri, and M. A. Zaïdi, "Electronic properties of multi-quantum dot structures in Cd 1-xZnxS alloy semiconductors," *Eur. Phys. J. B.*, vol. 53, pp. 35-38, 2006.

[13] A. Sakly, N. Safta, A. Mejri, H. Mejri, and A. Ben Lamine, "The excited electronic states calculated for Cd1-xZnxS quantum dots grown by the sol-gel technique," *J. Nanomater, ID746520*, 2010.

[14] A. Sakly, N. Safta, H. Mejri, and A. Ben Lamine, "The electronic band parameters calculated by the Kronig–Penney method for Cd 1-xZnxS quantum dot superlattices," *J. Alloys Compd.*, vol. 476, pp. 648-652, 2009.

[15] A. Sakly, N. Safta, H. Mejri, and A. Ben Lamine, "The electronic states calculated using the sinusoidal potential for Cd1-xZnxS quantum dot superlattices," *J. Alloys Compd.*, vol. 509, pp. 2493-2495, 2011.

[16] S. Marzougui and N. Safta, "The electronic band parameters calculated by the triangular potential model for Cd1-xZnxS quantum dot superlattices," *IOSR-JAP*, vol. 5, pp. 36-42, 2014.

[17] S. Marzougui and N. Safta, "The electronic band parameters calculated by the tight binding approximation for Cd1-xZnxS quantum dot superlattices," *IOSR-JAP*, vol. 6, pp. 15-21, 2014.

[18] S. Marzougui and N. Safta, "A theoretical study of the electronic properties of Cd1-xZnxS quantum dot superlattices," *American Journal of Nanoscience and Nanotechnology*, vol. 2, pp. 45-49, 2014.

[19] S. Marzougui and N. Safta, "A theoretical study of the heavy and light hole properties of Cd1-xZnxS quantum dot superlattices," *International Journal of Materials Science and Applications*, vol. 3, pp. 274-278, 2014.

[20] N.-K. Cho, J.-W. Yu, Y. H. Kim, and S. J. Kang, "Effect of oxygen plasma treatment on CdSe/CdZnS quantum-dot light-emitting diodes," *Jpn. J. Appl. Phys.*, vol. 53, p. 032101, 2014.

[21] Y. Wang, K. S. Leck, V. D. Ta, R. Chen, V. Nalla, Y. Gao, T. He, H. V. Demir, and H. Sun, "Blue liquid lasers from solution of CdZnS/ZnS ternary alloy quantum dots with quasi-continuous pumping," *Adv. Mater*, Doi: 10.1002/adma.201403237, 2014.

[22] J. J. Beato-López, C. Fernández-Ponce, E. Blanco, C. Barrera-Solano, M. Ramírez-del-Solar, M. Domínguez, F. García-Cozar, and R. Litrán, "Preparation and characterization of fluorescent CdS quantum dots used for the direct detection of GST fusion proteins," *Nanomaterials and Nanotechnology, Art*, vol. 2, p. 10, 2012.

[23] K. Deepa, S. Senthil, S. Shriprasad, and J. Madhavan, "CdS quantum dots sensitized solar cells," *International Journal of Chem Tech Research*, vol. 6, pp. 1956–1958, 2014.

[24] L. Cao, S. Huang, and E. S, "ZnS/CdS/ZnS quantum dot - quantum well produced in inverted micelles," *J. Colloid Interface Sci.*, vol. 273, pp. 478–482, 2004.

[25] H. Kumano, A. Ueta, and I. Suemune, "Modified spontaneous emission properties of CdS quantum dots embedded in novel three-dimensional microcavities," *Physica E.*, vol. 13, pp. 441-445, 2002.

[26] Y. C. Zhang, W. W. Chen, and X. Y. Hu, "In air synthesis of hexagonal Cd1-xZnxS nanoparticles from single-source molecular precursors," *Mater. Lett.*, vol. 61, pp. 4847-4850, 2007.

[27] K. Tomihira, D. Kim, and M. Nakayama, "Optical properties of ZnS-CdS alloy quantum dots prepared by a colloidal method," *J. Lumin.*, vol. 112, pp. 131- 135, 2005.

[28] C. S. Pathak, D. D. Mishra, V. Agarawala, and M. K. Mandal, "Mechanochemical synthesis, characterization and optical properties of zinc sulphide nanoparticles," *Indian J. Phys.*, vol. 86, pp. 777–781, 2012.

[29] S. Roy, A. Gogoi, and G. A. Ahmed, "Size dependent optical characterization of semiconductor particle: CdS embedded in polymer matrix," *Indian J. Phys.*, vol. 84, pp. 1405-1411, 2010.

[30] A. U. Ubale and A. N. Bargal, "Characterization of nanostructured photosensitive cadmium sulphide thin films grown by SILAR deposition technique," *Indian J. Phys.*, vol. 84, pp. 1497–1507, 2010.

[31] G. K. Padam, G. L. Mahotra, and S. U. M. Rao, "Studies on solution-grown thin films of Zn x Cd1−x S," *J. Appl. Phys.*, vol. 63, pp. 770-774, 1988.

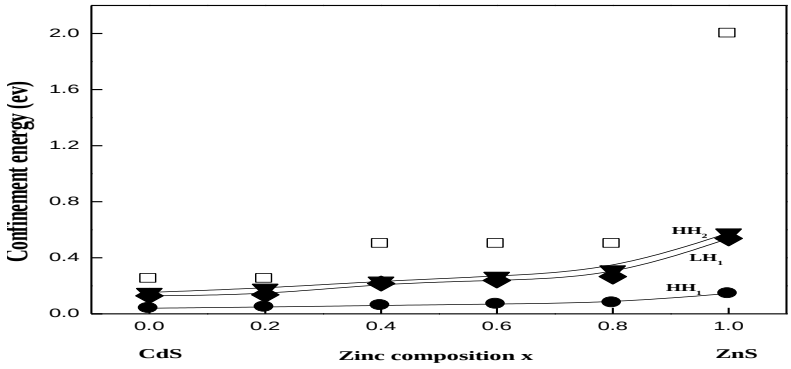

Figure-1. The sub bands HH_1, HH_2 and LH_1 calculated versus Zn composition x in $Cd_{1-x}Zn_xS$ QDs. The symbol □ indicates the potential barrier heights for holes.

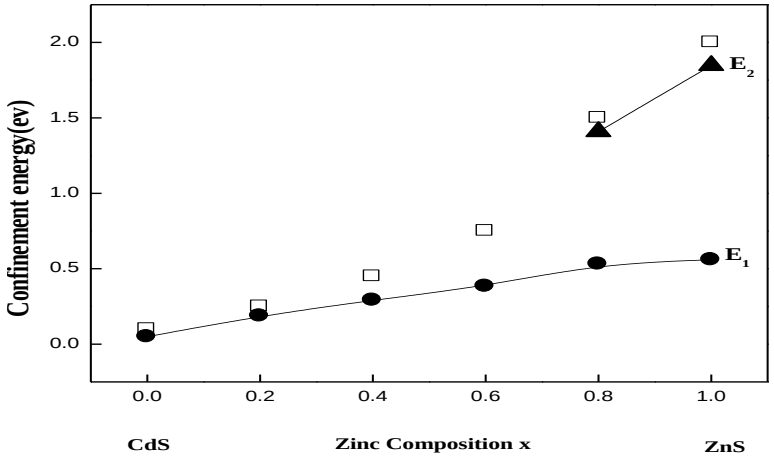

Figure-2. The sub bands E_1 and E_2 calculated as a function of Zn composition x in $Cd_{1-x}Zn_xS$ QDs. The symbol □ indicates the potential barrier heights for electrons.

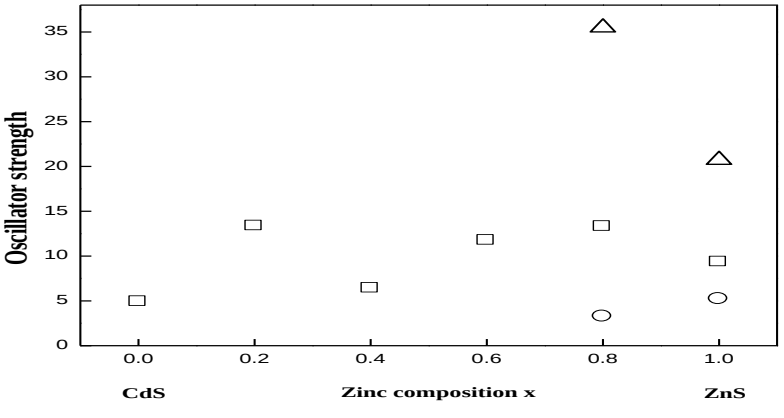

Figure-3. The x-dependent oscillator strength of inter sub band transitions in $Cd_{1-x}Zn_xS$ QDs:
□ $E_1 \rightarrow HH_2$; ○ $E_2 \rightarrow LH_1$; △ $\rightarrow HH_1$

Table-1. Parameters taken from Ref. [12] and used to calculate the sub band energies.

x	$\frac{m_e^*}{m_0}$	$\frac{m_h^*}{m_0}$	V_e(eV)	V_h(eV)	L (nm)
0.0	0.16	5.00	0.10	0.25	1.0
0.2			0.25	0.25	1.0
0.4			0.45	0.50	1.0
0.6			0.75	0.50	1.0
0.8			1.50	0.50	1.0
1.0	0.28	1.76	2.00	2.00	1.0

Table-2. The fit of the sub band energies versus composition as calculated for the electron and hole states in $Cd_{1-x}Zn_xS$ QDs.

State level	Polynomial law
E_1	$-0.493x^3+0.662x^2+0.302x+0.094$
HH_1	$0.256x^3-0.274x^2+0.117x+0.038$
HH_2	$1.210x^3-1.303x^2+0.516x+0.144$
LH_1	$1.211x^3-1.319x^2+0.516x+0.115$

Table-3. Values of E_g^{bulk} used in this work and taken from Ref. [27]

x	$E_g^{bulk}(eV)$
0.0	2.42
0.2	2.61
0.4	2.82
0.6	3.05
0.8	3.31
1.0	3.60